INTERNATIONAL JOURNAL FOR NUMERICAL METHODS IN FLUIDS
Int. J. Numer. Meth. Fluids 2008; **56**:1969–1991
Published online 17 July 2007 in Wiley InterScience (www.interscience.wiley.com). DOI: 10.1002/fld.1570

Time-domain BEM solution of convection–diffusion-type MHD equations

N. Bozkaya and M. Tezer-Sezgin*, †

Department of Mathematics, Middle East Technical University, 06531 Ankara, Turkey

SUMMARY

The two-dimensional convection–diffusion-type equations are solved by using the boundary element method (BEM) based on the time-dependent fundamental solution. The emphasis is given on the solution of magnetohydrodynamic (MHD) duct flow problems with arbitrary wall conductivity. The boundary and time integrals in the BEM formulation are computed numerically assuming constant variations of the unknowns on both the boundary elements and the time intervals. Then, the solution is advanced to the steady-state iteratively. Thus, it is possible to use quite large time increments and stability problems are not encountered. The time-domain BEM solution procedure is tested on some convection–diffusion problems and the MHD duct flow problem with insulated walls to establish the validity of the approach. The numerical results for these sample problems compare very well to analytical results. Then, the BEM formulation of the MHD duct flow problem with arbitrary wall conductivity is obtained for the first time in such a way that the equations are solved together with the coupled boundary conditions. The use of time-dependent fundamental solution enables us to obtain numerical solutions for this problem for the Hartmann number values up to 300 and for several values of conductivity parameter. Copyright © 2007 John Wiley & Sons, Ltd.

Received 8 February 2007; Revised 18 April 2007; Accepted 13 June 2007

KEY WORDS: BEM; MHD flow; time-dependent fundamental solution; convection–diffusion

1. INTRODUCTION

The boundary element method (BEM) has become increasingly popular in the numerical solution of time-dependent partial differential equations occurring in many branches of science and engineering. There are several different BEM approaches available for time-dependent problems as the Laplace transform method, dual reciprocity boundary element method (DRBEM) and the time-dependent fundamental solution method. The Laplace transform method needs the inverse transform to recover the solution. DRBEM results in a system of ordinary differential equations

*Correspondence to: M. Tezer-Sezgin, Department of Mathematics, Middle East Technical University, 06531 Ankara, Turkey.
†E-mail: munt@metu.edu.tr

to be solved by using another numerical scheme for the time derivative in the governing equation, and usually finite difference method (FDM) is chosen for the time integration. But, due to the stability problems very small time increment must be used and this is computationally expensive and time consuming.

The BEM applications of the time-dependent convection–diffusion problems are due to Grigoriev and Dargush [1–3]. In these studies, they have used time-dependent fundamental solution together with higher-order boundary elements. Linear, quadratic and quartic time interpolation functions are introduced for exact integrations which make the computations quite complex. Although, the efficiency of their BEM solutions increases with the increase of the Peclet number of the flow, they need to use small time steps. DeSilva *et al*. [4] have been attempted to develop a BEM formulation for transient conduction–convection problems involving spatially varying convective velocities. The fundamental solution corresponding to a transient conduction–convective problem with a constant velocity is utilized. The variable part of the convective velocity goes to the domain integral in this formulation.

The two-dimensional transient MHD flows in channels(ducts) are governed by coupled convection–diffusion-type equations for the velocity and the induced magnetic field. When the magnetic field is zero on the walls (insulated walls), the equations and the boundary conditions can be decoupled but for the arbitrary wall conductivity case the decoupling of the equations makes the boundary conditions coupled. Thus, it is quite difficult to treat the equations with BEM for arbitrary wall conductivity. The numerical solutions of time-dependent MHD flow equations have been given by Singh and Lal [5] in two dimensions and by Salah *et al*. [6] in three dimensions using finite element method (FEM). The time derivative was evaluated by a finite-difference-like expression. Seungsoo and Dulikravich [7] proposed an FDM scheme for three-dimensional unsteady MHD flow together with temperature field. They have used explicit Runge–Kutta method for step-by-step computations in time. Sheu and Lin [8] presented convection–diffusion–reaction model for solving unsteady MHD flow applying an FDM on non-staggered grids with a transport scheme in each ADI(predictor–corrector) spatial sweep. The solution algorithm in each of these unsteady MHD flow studies is based on explicit time-stepping schemes starting with the given initial conditions. Thus, the time increment must be taken very small to deal with the stability problems, and therefore they are computationally expensive. A numerical scheme which is a combination of the DRBEM in space and the differential quadrature method (DQM) in time has been proposed by Bozkaya and Tezer-Sezgin [9] for solving unsteady MHD flow problem in a rectangular duct with insulating walls. The solution procedure can be used with large time increments for obtaining the solution directly at the required time level. Computations have been carried out for moderate values of Hartmann number.

In this paper, fully transient solution procedure is performed using the BEM based on the time-dependent fundamental solution for convection–diffusion-type equations. Compared with DRBEM, FEM and FDM, less unwanted information about internal points is obtained using this approach. Since the fundamental solution is time dependent, time steps can be much larger than the finite difference time stepping. Constant variations of the solution and its normal derivative are used both on the boundary elements and on the time intervals and the integrals in the BEM formulation are evaluated numerically. Time integrals need higher-order numerical schemes for obtaining accurate solutions. The advantage of the solution procedure lies in taking quite large time steps for the computations and stability problems do not occur.

The main application of the proposed scheme is the solution of unsteady MHD flow problem in a rectangular duct with arbitrary wall conductivity. The algorithm is tested first on some

DOI: 10.1002/fld

convection–diffusion problems with Dirichlet and Neumann boundary conditions in which the exact solutions are available. The unsteady MHD duct flow problem with insulated walls is also included to establish the validity of the approach comparing the results with exact solution. For the MHD flow in a duct with arbitrary wall conductivity, the BEM formulation with time-dependent fundamental solution is presented for the two equations as a whole with coupled boundary conditions. This approach is particularly well suited for transient analysis of unsteady MHD flow problems. Solutions are obtained for values of Hartmann number up to 300 and for varying wall conductivity parameter. The well-known characteristics of the behaviour of MHD flow together with wall conductivity effect are presented in terms of velocity and induced magnetic field graphs.

2. BEM FORMULATION OF THE CONVECTION–DIFFUSION-TYPE EQUATIONS USING TIME-DEPENDENT FUNDAMENTAL SOLUTION

The governing equation for the time-dependent convection–diffusion-type problems can be expressed as

$$\frac{\partial T(\mathbf{x}, t)}{\partial t} + \mathbf{v} \cdot \nabla T(\mathbf{x}, t) = \kappa \nabla^2 T(\mathbf{x}, t), \quad \mathbf{x} \in \Omega, \ t > 0 \tag{1}$$

where $\mathbf{x} = (x, y)$ are spatial coordinates, $\mathbf{v} = (v_1, v_2)$ are the velocity components of the flow and $\kappa = 1/Pe$ is the diffusivity constant, Pe is the Peclet number.

This equation represents an initial-boundary value problem for the temperature $T(\mathbf{x}, t)$ with the given initial condition

$$T(\mathbf{x}, 0) = T_0(\mathbf{x}) \quad \text{at } t = 0 \quad \text{for } \mathbf{x} \in \Omega \tag{2}$$

and the given Dirichlet- and Neumann-type boundary conditions

$$\begin{aligned} T(\mathbf{x}, t) &= \bar{T}(\mathbf{x}, t) \quad \text{on } \mathbf{x} \in \Gamma_1 \\ \frac{\partial T}{\partial n}(\mathbf{x}, t) &= \bar{q}(\mathbf{x}, t) \quad \text{on } \mathbf{x} \in \Gamma_2 \end{aligned} \tag{3}$$

where $\Gamma = \Gamma_1 + \Gamma_2$ is the boundary of the domain $\Omega \subset R^2$ and $\mathbf{n} = (n_1, n_2)$ is the outward normal. $T_0(\mathbf{x})$, $\bar{T}(\mathbf{x}, t)$ and $\bar{q}(\mathbf{x}, t)$ are given functions.

The BEM is applied to Equation (1) for representing it in an equivalent boundary integral equation by using the time-dependent fundamental solution [1].

The 2D time-dependent fundamental solution of Equation (1) is of the form [10]

$$T^*(\xi, \tau; \mathbf{x}, t) = \frac{H[\tau - t]}{4\kappa\pi(\tau - t)} \mathrm{e}^{(-|\mathbf{x} - \xi + \mathbf{v}(\tau - t)|^2 / 4\kappa(\tau - t))} \tag{4}$$

where $\xi = (\xi_1, \xi_2)$ and $\mathbf{x} = (x, y)$ are the source (fixed) and field (variable) points in Ω, τ and t are the maximum time and time variation, respectively. H denotes the Heaviside function.

Now the method of weighted residuals [11] gives

$$\int_0^\tau \int_\Omega \left(\frac{\partial T}{\partial t} + \mathbf{v} \cdot \nabla T - \kappa \nabla^2 T \right) T^* \, \mathrm{d}\Omega \, \mathrm{d}t = 0 \tag{5}$$

DOI: 10.1002/fld

Integrating by parts the first-order time and space derivatives, assuming the flow has constant velocity components and using Green's second identity for the Laplacian part we obtain

$$-\int_0^\tau \int_\Omega \left(\frac{\partial T^*}{\partial t} + \mathbf{v} \cdot \nabla T^* + \kappa \nabla^2 T^* \right) T \, \mathrm{d}\Omega \, \mathrm{d}t + \int_\Omega (T\, T^*|_{t=\tau} - T\, T^*|_{t=0}) \, \mathrm{d}\Omega$$
$$+ \int_0^\tau \int_\Gamma \left\{ \mathbf{v}_n T\, T^* - \kappa T^* \frac{\partial T}{\partial n} + \kappa T \frac{\partial T^*}{\partial n} \right\} \mathrm{d}\Gamma \, \mathrm{d}t = 0 \tag{6}$$

where $\mathbf{v}_n = \mathbf{v} \cdot \mathbf{n} = v_1 n_1 + v_2 n_2$.

The fundamental solution T^* satisfies

$$T^*(\xi, \tau; \mathbf{x}, t) = 0 \quad \text{when } t \geqslant \tau \tag{7}$$

because of the property of the Heaviside function and also it is provided to satisfy the adjoint of Equation (1), i.e.

$$\frac{\partial T^*}{\partial t}(\xi, \tau; \mathbf{x}, t) + \mathbf{v} \cdot \nabla T^*(\xi, \tau; \mathbf{x}, t) + \kappa \nabla^2 T^*(\xi, \tau; \mathbf{x}, t) = -\Delta(\xi - \mathbf{x})\Delta(\tau - t) \tag{8}$$

where Δ is the Dirac delta function.

Thus, substitution of (7) and (8) into Equation (6) with the property of Dirac delta function gives

$$c(\xi) T(\xi, \tau) + \int_0^\tau \int_\Gamma \left\{ \mathbf{v}_n T^*(\xi, \tau; \mathbf{x}, t) + \kappa \frac{\partial T^*}{\partial n}(\xi, \tau; \mathbf{x}, t) \right\} T(\mathbf{x}, t) \, \mathrm{d}\Gamma \, \mathrm{d}t$$
$$= \int_0^\tau \int_\Gamma \kappa T^*(\xi, \tau; \mathbf{x}, t) \frac{\partial T}{\partial n}(\mathbf{x}, t) \, \mathrm{d}\Gamma \, \mathrm{d}t + \int_\Omega T(\mathbf{x}, 0) T^*(\xi, \tau; \mathbf{x}, 0) \, \mathrm{d}\Omega \tag{9}$$

where

$$c(\xi) = \begin{cases} 1 - \dfrac{\alpha}{2\pi} & \text{if } \xi \in \Gamma \\ 1 & \text{if } \xi \in \Omega - \Gamma \end{cases} \tag{10}$$

α being the internal angle at the point ξ.

The boundary Γ is discretized by using N constant boundary elements. The contributions from a source point to a field point used in the BEM discretization are shown in Figure 1(a) with the distance functions $\mathbf{r}_{in} = |\mathbf{x}_n - \xi^i|$ and $\mathbf{r}_{jn} = |\mathbf{x}_n - \xi^j|$. Figure 1(b) presents the mesh obtained by using N (e.g. $N = 20$) boundary nodes and a uniform collocation of $(N/4)^2$ (e.g. $(N/4)^2 = 25$) internal points. The time interval $[0, \tau]$ is divided into M subintervals. We assume constant variation for T and its normal derivative on each time step $[t_{m-1}, t_m]$ and over each boundary element Γ_n such that

$$T(\mathbf{x}, t) \approx T(\mathbf{x}_n, t_m) = T_n(t_m)$$
$$\frac{\partial T}{\partial n}(\mathbf{x}, t) \approx \frac{\partial T}{\partial n}(\mathbf{x}_n, t_m) = \left(\frac{\partial T}{\partial n} \right)_n (t_m) \tag{11}$$

DOI: 10.1002/fld

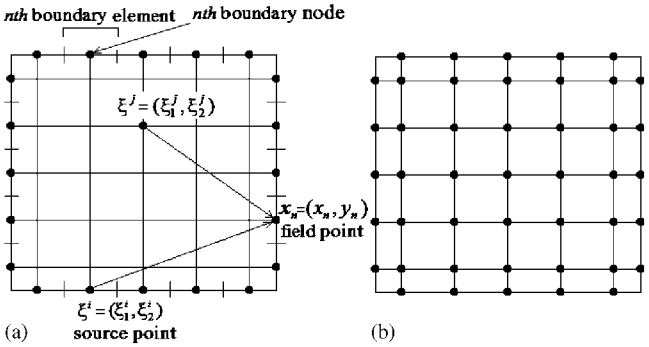

Figure 1. (a) Contributions from a source point to a field point. (b) Discretization of the domain Ω with constant boundary elements with a uniform grid density.

where $\mathbf{x}_n$ denotes the centre of the nth boundary element. Then, integral equation (9) yields

$$c_i T_i(t_m) + \sum_{n=1}^{N} T_n(t_m) \int_{t_{m-1}}^{t_m} \int_{\Gamma_n} \left(\mathbf{v}_n T^*(\xi^i, t_m; \mathbf{x}, t) + \kappa \frac{\partial T^*}{\partial n}(\xi^i, t_m; \mathbf{x}, t) \right) \mathrm{d}\Gamma_n \, \mathrm{d}t$$
$$= \sum_{n=1}^{N} \left(\frac{\partial T}{\partial n} \right)_n (t_m) \int_{t_{m-1}}^{t_m} \int_{\Gamma_n} \kappa T^*(\xi^i, t_m; \mathbf{x}, t) \, \mathrm{d}\Gamma_n \, \mathrm{d}t$$
$$+ \int_{\Omega} T(\mathbf{x}, t_{m-1}) T^*(\xi^i, t_m; \mathbf{x}, t_{m-1}) \, \mathrm{d}\Omega \tag{12}$$

for one boundary node ξ^i. Now ranging i and n from 1 to N (for each fixed choice of source point $\xi^i = (\xi_1^i, \xi_2^i)$ from 1 to N and ranging the field point $\mathbf{x}_n = (x_n, y_n)$ also from 1 to N), we obtain an $N \times N$ linear system of algebraic equations

$$H\{T\} - G\left\{ \frac{\partial T}{\partial n} \right\} = F \tag{13}$$

The entries of matrices H, G and vector F are given as

$$H_{in} = \int_{t_{m-1}}^{t_m} \int_{\Gamma_n} \left(\mathbf{v}_n T_i^* + \kappa \left(\frac{\partial T^*}{\partial n} \right)_i \right) \mathrm{d}\Gamma_n \, \mathrm{d}t + \frac{1}{2}\delta_{in}$$
$$G_{in} = \int_{t_{m-1}}^{t_m} \int_{\Gamma_n} \kappa T_i^* \, \mathrm{d}\Gamma_n \, \mathrm{d}t \tag{14}$$
$$F_i = \int_{\Omega} T(\mathbf{x}, t_{m-1}) \, T_i^* \Big|_{t=t_{m-1}} \mathrm{d}\Omega$$

where

$$T_i^* = T^*(\xi^i, t_m; \mathbf{x}, t)$$
$$\left(\frac{\partial T^*}{\partial n} \right)_i = \frac{\partial T}{\partial n}(\xi^i, t_m; \mathbf{x}, t)$$

DOI: 10.1002/fld

in two-dimensional space and δ is the Kronecker delta function. The substitution of the given boundary conditions (3) into Equation (13) results in a linear system of equations

$$Ax = b \tag{15}$$

which can be solved by Gaussian elimination for the unknown vector x. Here, x contains the unknown T and $\partial T/\partial n$ values on the boundary. Then, these boundary values are used in Equation (12) by taking $c_i = 1$, to compute T values at each interior point,

$$T_i(t_m) = -\sum_{n=1}^{N} \bar{H}_{in}\, T_n(t_m) + \sum_{n=1}^{N} G_{in} \left(\frac{\partial T}{\partial n}\right)_n (t_m) + F_i \tag{16}$$

where

$$\bar{H}_{in} = \int_{t_{m-1}}^{t_m} \int_{\Gamma_n} \left(\mathbf{v}_n T_i^* + \kappa \left(\frac{\partial T^*}{\partial n}\right)_i\right) \mathrm{d}\Gamma_n \,\mathrm{d}t$$

This time the contributions in the entries (the distance $|\mathbf{x}_n - \xi^i|$) will be from an interior node $\xi^i = (\xi_1^i, \xi_2^i)$ to the nth boundary element.

3. BEM APPLICATION TO THE MHD DUCT FLOW EQUATIONS

We consider the unsteady, laminar flow of an incompressible, viscous and electrically conducting fluid driven by a constant applied pressure gradient in a rectangular duct. The axis of the duct is chosen as the z-axis. A uniform magnetic field of strength (intensity, inductance) B_0 is imposed along the x-axis. The fluid motion is fully developed (i.e. the duct is assumed to be of infinite length and end effects are neglected). It is assumed that the sides of the duct are electrically insulated or have variable conductivity.

The basic equations governing the MHD duct flow have been obtained from Maxwell's equations of the electromagnetic field, Ohm's law, equation of continuity and the Navier–Stokes equations [12]. There is only one component $V_z(x, y, t)$ of the velocity field and one component $B_z(x, y, t)$ of the induced magnetic field in the z-direction. All physical quantities except pressure are independent of z, the magnetic field vector takes the form $B = (B_0, 0, B_z(x, y, t))$. We also assume that displacement currents are negligible. Thus, the z components of the governing equations become

$$\begin{aligned} \nabla^2 B_z + \sigma\mu_e B_0 \frac{\partial V_z}{\partial x} &= 0 \\ \mu\nabla^2 V_z + \frac{B_0}{\mu_e}\frac{\partial B_z}{\partial x} &= \frac{\partial p}{\partial z} \end{aligned} \tag{17}$$

where σ, μ are the electrical conductivity and the coefficients of viscosity of the fluid, respectively. μ_e is the magnetic permeability and p is the pressure. So the partial differential equations (in non-dimensional form) in terms of velocity $V(x, y, t)$ and induced magnetic field $B(x, y, t)$ are

$$\begin{aligned} \nabla^2 V + M\frac{\partial B}{\partial x} &= -1 + \frac{\partial V}{\partial t} \\ \nabla^2 B + M\frac{\partial V}{\partial x} &= \frac{\partial B}{\partial t} \end{aligned} \tag{18}$$

DOI: 10.1002/fld

where non-dimensionalization was performed with a characteristic length L_0 and a characteristic velocity V_0 (mean axis velocity). The dimensionless variables are

$$V = \frac{V_z}{V_0}, \quad B = \frac{\sigma\mu^{-1/2} B_z}{V_0 \mu_e}, \quad V_0 = \frac{-L_0^2(\partial p/\partial z)}{\mu}$$

and M is the Hartmann number given by

$$M = \frac{B_0 L_0 \sqrt{\sigma}}{\sqrt{\mu}}$$

Now the BEM approach, given for the general convection–diffusion-type equations in Section 2, is used to solve the unsteady MHD flow problem in a square duct with insulating walls or with variable conductivity on the walls. First, we present the BEM application to the unsteady MHD flow problem in a square duct with insulated walls, which has an exact solution.

3.1. MHD flow in a rectangular duct with insulated walls

The non-dimensional equations of the unsteady, laminar, viscous flow of an incompressible and electrically conducting fluid, in terms of the velocity V and the induced magnetic field B are

$$\begin{aligned} \nabla^2 V + M\frac{\partial B}{\partial x} &= -1 + \frac{\partial V}{\partial t} \\ \nabla^2 B + M\frac{\partial V}{\partial x} &= \frac{\partial B}{\partial t} \end{aligned} \tag{19}$$

in the rectangular section Ω of a duct with the boundary and initial conditions

$$\begin{aligned} V(x, y, t) = 0, \quad B(x, y, t) = 0 \quad (x, y) \in \partial\Omega \\ V(x, y, 0) = 0, \quad B(x, y, 0) = 0 \quad (x, y) \in \Omega \end{aligned} \tag{20}$$

If we make the change of variables

$$U_1 = V + B, \quad U_2 = V - B \tag{21}$$

the MHD equations in (19) can be decoupled as

$$\begin{aligned} \nabla^2 U_1 + M\frac{\partial U_1}{\partial x} &= -1 + \frac{\partial U_1}{\partial t} \\ \nabla^2 U_2 - M\frac{\partial U_2}{\partial x} &= -1 + \frac{\partial U_2}{\partial t} \end{aligned} \quad (x, y, t) \in \Omega \times [0, \infty) \tag{22}$$

with the corresponding boundary and initial conditions

$$\begin{aligned} U_1(x, y, t) = 0, \quad U_2(x, y, t) = 0 \quad (x, y) \in \partial\Omega \\ U_1(x, y, 0) = 0, \quad U_2(x, y, 0) = 0 \quad (x, y) \in \Omega \end{aligned} \tag{23}$$

A further simplification by the transformations

$$MU_1 = MW_1 - x, \quad MU_2 = MW_2 + x \tag{24}$$

DOI: 10.1002/fld

results in two initial and boundary value problems

$$\begin{aligned} &\frac{\partial W_1}{\partial t} - M\frac{\partial W_1}{\partial x} = \nabla^2 W_1 \quad \text{in } \Omega, \qquad \frac{\partial W_2}{\partial t} + M\frac{\partial W_2}{\partial x} = \nabla^2 W_2 \quad \text{in } \Omega \\ &W_1(x, y, t) = \frac{x}{M} \quad \text{on } \partial\Omega, \qquad W_2(x, y, t) = -\frac{x}{M} \quad \text{on } \partial\Omega \\ &W_1(x, y, 0) = \frac{x}{M}, \qquad W_2(x, y, 0) = -\frac{x}{M} \end{aligned} \tag{25}$$

Now, the BEM approach in Section 2 can be applied to these convection–diffusion-type problems.

The decoupled equations in (25) can be weighted as

$$\begin{aligned} &\int_0^\tau \int_\Omega \left(\frac{\partial W_1}{\partial t} - M\frac{\partial W_1}{\partial x} - \nabla^2 W_1 \right) W_1^* \, \mathrm{d}\Omega \, \mathrm{d}t = 0 \\ &\int_0^\tau \int_\Omega \left(\frac{\partial W_2}{\partial t} + M\frac{\partial W_2}{\partial x} - \nabla^2 W_2 \right) W_2^* \, \mathrm{d}\Omega \, \mathrm{d}t = 0 \end{aligned} \tag{26}$$

where W_1^* and W_2^* are the corresponding time-dependent fundamental solutions obtained from (4), i.e.

$$\begin{aligned} W_1^*(\xi, \tau; \mathbf{x}, t) &= \frac{H[\tau - t]}{4\pi(\tau - t)} \mathrm{e}^{(-|\mathbf{x}-\xi+\mathbf{u}(\tau-t)|^2/4(\tau-t))} \\ W_2^*(\xi, \tau; \mathbf{x}, t) &= \frac{H[\tau - t]}{4\pi(\tau - t)} \mathrm{e}^{(-|\mathbf{x}-\xi+\mathbf{v}(\tau-t)|^2/4(\tau-t))} \end{aligned} \tag{27}$$

which are only differing in the coefficients $\mathbf{u} = (-M, 0)$ and $\mathbf{v} = (M, 0)$, respectively. $\xi = (\xi_1, \xi_2)$ and $\mathbf{x} = (x, y)$ are the source (fixed) and field (variable) points in Ω. The source and field points may vary from boundary nodes to boundary elements, whereas for the interior computations source point is taken inside of the domain Ω.

Applying integration by parts and Green's second identity to the equations in (26), one can obtain the boundary integral equations

$$\begin{aligned} &c(\xi) W_1(\xi, \tau) + \int_0^\tau \int_\Gamma \left(\mathbf{u}_n W_1^* + \frac{\partial W_1^*}{\partial n} \right) W_1(\mathbf{x}, t) \, \mathrm{d}\Gamma \, \mathrm{d}t \\ &\quad = \int_0^\tau \int_\Gamma W_1^* \frac{\partial W_1}{\partial n}(\mathbf{x}, t) \, \mathrm{d}\Gamma \, \mathrm{d}t + \int_\Omega W_1(\mathbf{x}, 0) W_1^*(\xi, \tau; \mathbf{x}, 0) \, \mathrm{d}\Omega \end{aligned} \tag{28}$$

$$\begin{aligned} &c(\xi) W_2(\xi, \tau) + \int_0^\tau \int_\Gamma \left(\mathbf{v}_n W_2^* + \frac{\partial W_2^*}{\partial n} \right) W_2(\mathbf{x}, t) \, \mathrm{d}\Gamma \, \mathrm{d}t \\ &\quad = \int_0^\tau \int_\Gamma W_2^* \frac{\partial W_2}{\partial n}(\mathbf{x}, t) \, \mathrm{d}\Gamma \, \mathrm{d}t + \int_\Omega W_2(\mathbf{x}, 0) W_2^*(\xi, \tau; \mathbf{x}, 0) \, \mathrm{d}\Omega \end{aligned} \tag{29}$$

where $\mathbf{u}_n = \mathbf{u} \cdot \mathbf{n} = -Mn_1$ and $\mathbf{v}_n = \mathbf{v} \cdot \mathbf{n} = Mn_1$.

DOI: 10.1002/fld

Then, the discretization of the boundary with N constant boundary elements given in Figure 1 with the assumption of constant variations for W_1 and W_2 and their normal derivatives along each time interval $[t_{m-1}, t_m]$ gives the following discretized equations:

$$c_i W_{1i}(t_m) + \sum_{n=1}^{N} W_{1n}(t_m) \int_{t_{m-1}}^{t_m} \int_{\Gamma_n} \left(\mathbf{u}_n W_{1i}^* + \frac{\partial W_{1i}^*}{\partial n} \right) \mathrm{d}\Gamma_n \, \mathrm{d}t$$

$$= \sum_{n=1}^{N} \left(\frac{\partial W_1}{\partial n} \right)_n (t_m) \int_{t_{m-1}}^{t_m} \int_{\Gamma_n} W_{1i}^* \, \mathrm{d}\Gamma_n \, \mathrm{d}t + \int_{\Omega} W_1(\mathbf{x}, t_{m-1}) W_1^*(\xi^i, t_m; \mathbf{x}, t_{m-1}) \, \mathrm{d}\Omega \quad (30)$$

$$c_i W_{2i}(t_m) + \sum_{n=1}^{N} W_{2n}(t_m) \int_{t_{m-1}}^{t_m} \int_{\Gamma_n} \left(\mathbf{v}_n W_{2i}^* + \frac{\partial W_{2i}^*}{\partial n} \right) \mathrm{d}\Gamma_n \, \mathrm{d}t$$

$$= \sum_{n=1}^{N} \left(\frac{\partial W_2}{\partial n} \right)_n (t_m) \int_{t_{m-1}}^{t_m} \int_{\Gamma_n} W_{2i}^* \, \mathrm{d}\Gamma_n \, \mathrm{d}t + \int_{\Omega} W_2(\mathbf{x}, t_{m-1}) W_2^*(\xi^i, t_m; \mathbf{x}, t_{m-1}) \, \mathrm{d}\Omega \quad (31)$$

Thus, we obtain the $N \times N$ linear system of equations

$$H\{W_1\} - G\left\{ \frac{\partial W_1}{\partial n} \right\} = F \quad (32)$$

$$\widetilde{H}\{W_2\} - \widetilde{G}\left\{ \frac{\partial W_2}{\partial n} \right\} = \widetilde{F} \quad (33)$$

where the entries of the coefficient matrices $H, G, \widetilde{H}, \widetilde{G}$ and right-hand-side vectors $F, \widetilde{F}$ are similarly defined as in (14). The insulated boundary conditions $W_1 = x/M$ and $W_2 = -x/M$ are inserted to systems (32) and (33) by rearranging the equations to include the known values to the right-hand sides of the equations. This yields the linear system of algebraic equations

$$Ax = b \quad (34)$$

$$\widetilde{A}\widetilde{x} = \widetilde{b} \quad (35)$$

where x contains the unknown $\partial W_1/\partial n$ values and $\widetilde{x}$ contains the unknown $\partial W_2/\partial n$ values on the boundary. All the known boundary information are combined with the vectors F and $\tilde{F}$ forming the right-hand sides b and $\tilde{b}$. The solution of the final systems give the required unknowns $\partial W_1/\partial n$ and $\partial W_2/\partial n$ on the boundary. We take $c_i = 1$ in the discretized Equations (30) and (31) in order to compute W_1 and W_2 at the interior points. Then, one can obtain the original unknowns V and B by backward substitution through transformations (24) and (21).

3.2. MHD flow in a rectangular duct having variable wall conductivity

Having variable electrical conductivity on the walls of the duct means we have mixed-type boundary conditions for the magnetic field, i.e.

$$\frac{\partial B}{\partial n} + \lambda B = 0 \quad (36)$$

DOI: 10.1002/fld

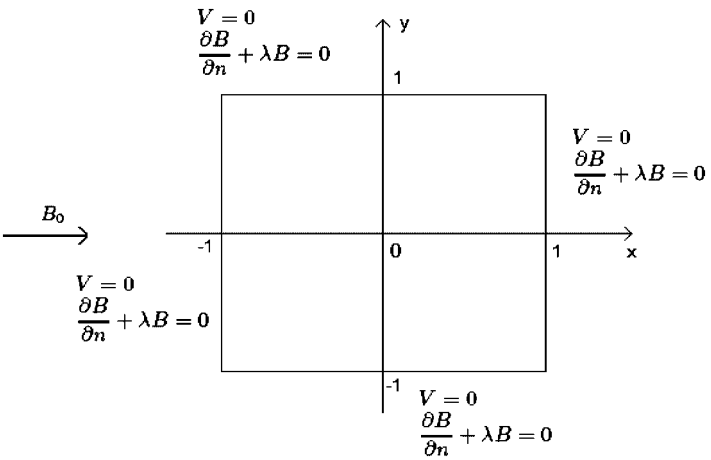

Figure 2. Square section of the duct with variable wall conductivity.

on the boundary of the flow region shown in Figure 2. When $\lambda = 0$, the walls are perfectly conducting, when $\lambda \to \infty$ the walls are insulated. For the other values of $\lambda > 0$, the walls are having variable electrical conductivity. Therefore, this unsteady MHD duct flow problem is also defined by the non-dimensional Equations (19):

$$\begin{aligned} \nabla^2 V + M\frac{\partial B}{\partial x} &= -1 + \frac{\partial V}{\partial t} \\ \nabla^2 B + M\frac{\partial V}{\partial x} &= \frac{\partial B}{\partial t} \end{aligned} \tag{37}$$

with the zero initial conditions

$$V(x, y, 0) = 0, \quad B(x, y, 0) = 0 \quad (x, y) \in \Omega \tag{38}$$

and the zero boundary condition for velocity and the mixed-type boundary condition for the induced magnetic field

$$V(x, y, t) = 0, \quad \frac{\partial B}{\partial n}(x, y, t) + \lambda B(x, y, t) = 0 \quad (x, y) \in \partial\Omega \tag{39}$$

Now using the transformations in (21) and (24), one can obtain the decoupled form of the equations in (37) in terms of W_1 and W_2

$$\begin{aligned} \frac{\partial W_1}{\partial t} - M\frac{\partial W_1}{\partial x} - \nabla^2 W_1 &= 0 \\ \frac{\partial W_2}{\partial t} + M\frac{\partial W_2}{\partial x} - \nabla^2 W_2 &= 0 \end{aligned} \tag{40}$$

with the decoupled initial conditions

$$W_1(x, y, 0) = \frac{x}{M}, \quad W_2(x, y, 0) = \frac{-x}{M} \quad (x, y) \in \Omega \tag{41}$$

DOI: 10.1002/fld

But this time, we have coupled boundary conditions such that

$$W_1 + W_2 = 0$$
$$\frac{\partial W_2}{\partial n} - \frac{\partial W_1}{\partial n} = \lambda(W_1 - W_2) - \frac{2}{M}\frac{\partial x}{\partial n} - 2\lambda\frac{x}{M} \quad \text{on } \partial\Omega \tag{42}$$

because of the mixed-type boundary condition for the induced magnetic field.

However, we can still apply the BEM using the time-dependent fundamental solution to the resulting equations in (40) which are defining two convection–diffusion-type equations. Thus, the BEM applications result in the same linear system of equations as (32) and (33):

$$H\{W_1\} - G\left\{\frac{\partial W_1}{\partial n}\right\} = F \tag{43}$$

$$\widetilde{H}\{W_2\} - \widetilde{G}\left\{\frac{\partial W_2}{\partial n}\right\} = \widetilde{F} \tag{44}$$

Since the boundary conditions are coupled, we do not know directly neither W_1 and W_2 nor their normal derivatives on the boundary. Thus, the $N \times N$ systems in (43) and (44) cannot be converted into $Ax = b$ and $\widetilde{A}\widetilde{x} = \widetilde{b}$ forms as in the insulated wall case explained in Section 3.2. Then, we observe that the final systems should have to be solved together by using the coupled boundary conditions and we present a new solution procedure in this sense.

When the boundary conditions in (42) are substituted in (44), one can obtain

$$-\widetilde{H}\{W_1\} - \widetilde{G}\left\{\frac{\partial W_1}{\partial n}\right\} - 2\lambda\widetilde{G}\{W_1\} + \frac{2}{M}\widetilde{G}\left\{\frac{\partial x}{\partial n} + \lambda x\right\} = \widetilde{F} \tag{45}$$

and it can be rewritten as

$$(-\widetilde{H} - 2\lambda\widetilde{G})\{W_1\} - \widetilde{G}\left\{\frac{\partial W_1}{\partial n}\right\} = \widetilde{F} - \frac{2}{M}\widetilde{G}\left\{\frac{\partial x}{\partial n} + \lambda x\right\} \tag{46}$$

In this system, $\{\partial x/\partial n + \lambda x\}$ is an $N \times 1$ vector of which entries are functions of x and can be computed easily at the boundary nodes. Thus, the right-hand side of Equation (46) is known but on the left-hand side of the equation, we have two unknown vectors $\{W_1\}$ and $\{\partial W_1/\partial n\}$ as in Equation (43). Now the systems in (43) and (46) are combined in such a way that we have a linear system of the form $Ax = b$ at the end

$$\left[\begin{array}{c|c} H & -G \\ \hline -\widetilde{H} - 2\lambda\widetilde{G} & -\widetilde{G} \end{array}\right]_{2N\times 2N} \left[\begin{array}{c} W_1 \\ \hline \dfrac{\partial W_1}{\partial n} \end{array}\right]_{2N\times 1} = \left[\begin{array}{c} F \\ \hline \widetilde{F} - \dfrac{2}{M}\widetilde{G}\left\{\dfrac{\partial x}{\partial n} + \lambda x\right\} \end{array}\right]_{2N\times 1} \tag{47}$$

Finally, we solve the $2N \times 2N$ system above for W_1 and its normal derivative on the boundary by using a solver which uses the LU factorization of the coefficient matrix based on Gauss elimination

DOI: 10.1002/fld

with partial pivoting. Then by using relationship (42), W_2 and its normal derivative are computed on the boundary. For the internal values of W_1 and W_2, we make use of Equations (30) and (31) as explained in Section 3.1. Then, the transformations (21) and (24) give the required unknowns V and B in Ω in turn.

4. NUMERICAL RESULTS AND DISCUSSION

4.1. Convection–diffusion-type problems

We first consider two convection–diffusion problems for testing the accuracy of our solution procedure. The domain of the first problem is a unit square in the (x, y)-plane with the Dirichlet-type boundary conditions. The second problem is defined in a rectangular region $0 \leqslant x \leqslant 1$ and $0 \leqslant y \leqslant 0.7$ and it is solved with Dirichlet- and Neumann-type boundary conditions. All integrations appearing in the entries of the BEM matrices are computed numerically by using Gauss Legendre integration with 16–64 points. The solutions are obtained at steady state, which is reached when the absolute difference between the solutions of two consecutive time levels is less than 10^{-5} and they are compared with the available steady-state exact solutions. The computations are carried out by using only 20 constant boundary elements and interior values are obtained for presenting the solutions in terms of graphics. Comparing to other time integration methods, we are able to use quite large time increments (e.g. $\Delta t = 1.0, 2.0$) in this procedure since the time-dependent fundamental solution is used.

4.1.1. Problem 1 (Grigoriev and Dargush [3]). We solve the convection–diffusion equation

$$\frac{\partial T}{\partial t} + \frac{\partial T}{\partial x} + \frac{1}{2}\frac{\partial T}{\partial y} = \nabla^2 T, \quad 0 \leqslant x \leqslant 1,\ 0 \leqslant y \leqslant 1,\ t > 0$$

with the non-zero initial condition

$$T(x, y, 0) = \exp(-((x + 1/4)^2 + y^2)/4)$$

and the time-dependent Dirichlet-type boundary conditions

$$T(0, y, t) = \frac{1}{1+t}\exp[-((1/4 - t)^2 + (y - t/2)^2)/(4(1 + t))], \quad 0 < y < 1$$

$$T(1, y, t) = \frac{1}{1+t}\exp[-((5/4 - t)^2 + (y - t/2)^2)/(4(1 + t))], \quad 0 < y < 1$$

$$T(x, 0, t) = \frac{1}{1+t}\exp[-((x - t + 1/4)^2 + (t/2)^2)/(4(1 + t))], \quad 0 < x < 1$$

$$T(x, 1, t) = \frac{1}{1+t}\exp[-((x - t + 1/4)^2 + (1 - t/2)^2)/(4(1 + t))], \quad 0 < x < 1$$

DOI: 10.1002/fld

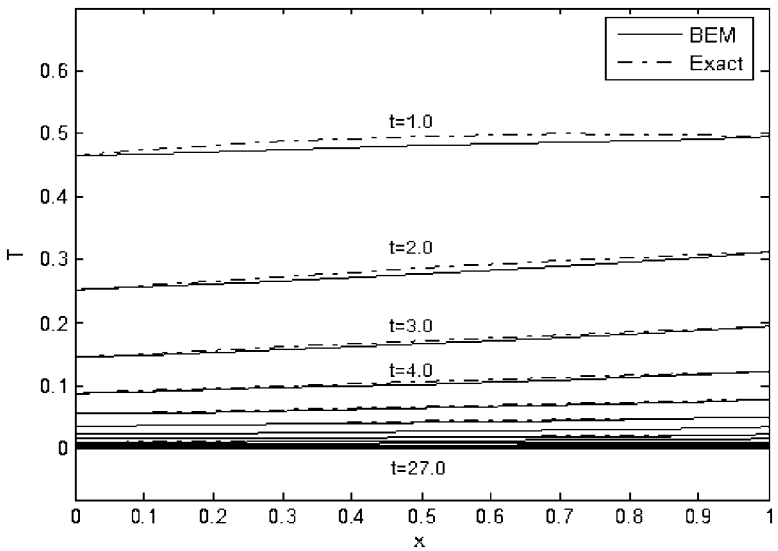

Figure 3. Solution of the convection–diffusion problem 1 at $y = 0.5$ with $\Delta t = 1.0$.

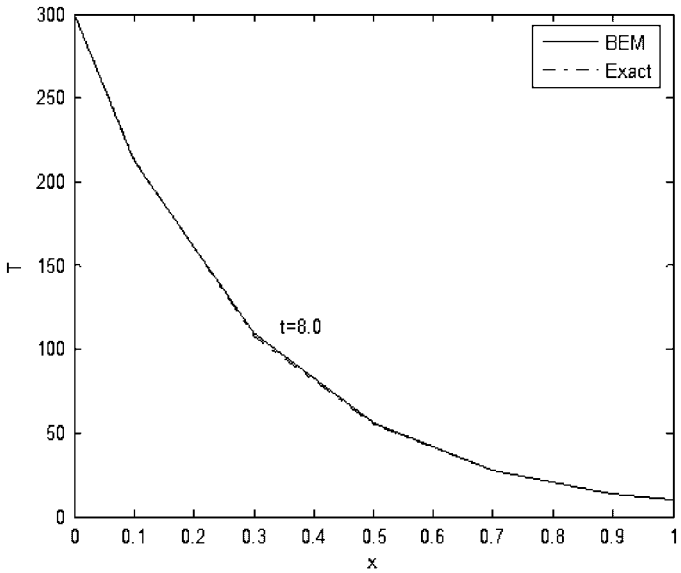

Figure 4. Solution of the convection–diffusion problem 2 at $y = 0.35$ with $\Delta t = 2.0$.

The exact solution is given by

$$T(x, y, t) = \frac{1}{1+t} \exp[-((x - t + 1/4)^2 + (y - t/2)^2)/(4(1+t))]$$

DOI: 10.1002/fld

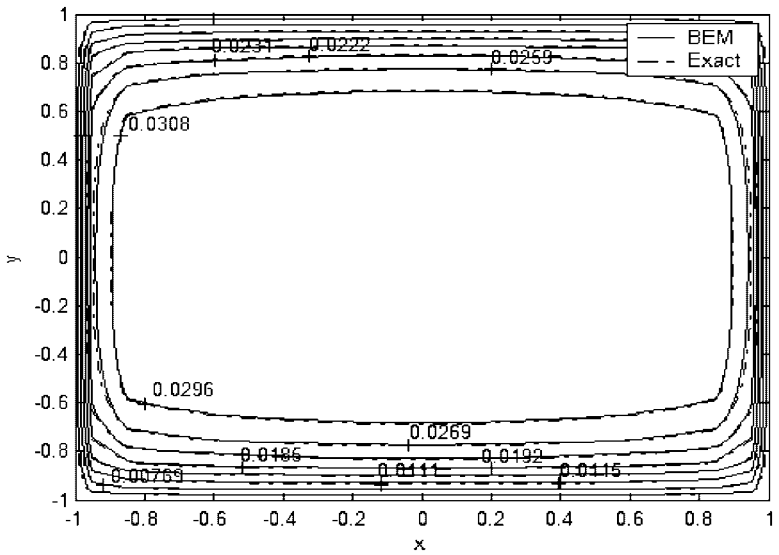

Figure 5. Velocity for $M = 30$, $\tau = 1.2$.

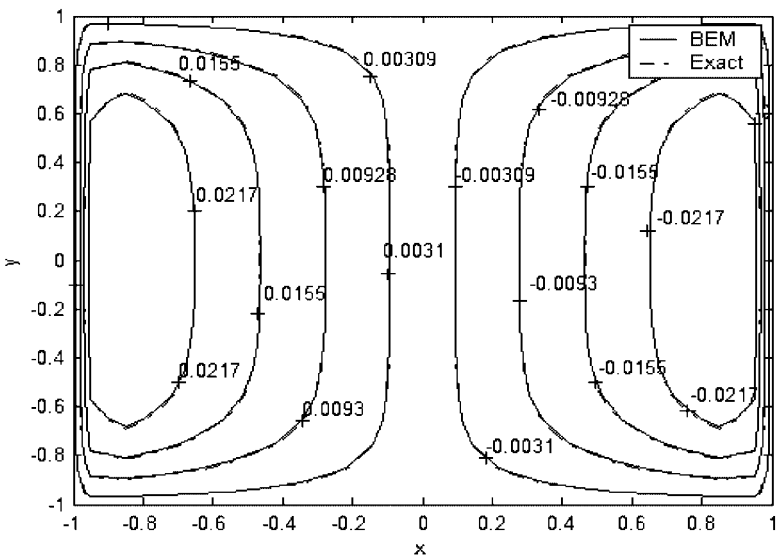

Figure 6. Induced magnetic field for $M = 30$, $\tau = 1.2$.

The boundary of the square region $[0, 1] \times [0, 1]$ is discretized with 20 constant boundary elements and 25 equally spaced interior points. Figure 3 shows the behaviour of the solution at $y = 0.5$ along the x-direction at several time levels. After 27 time steps with the time increment $\Delta t = 1.0$, the solution approaches the steady state, which is zero, in a good agreement with the exact solution.

DOI: 10.1002/fld

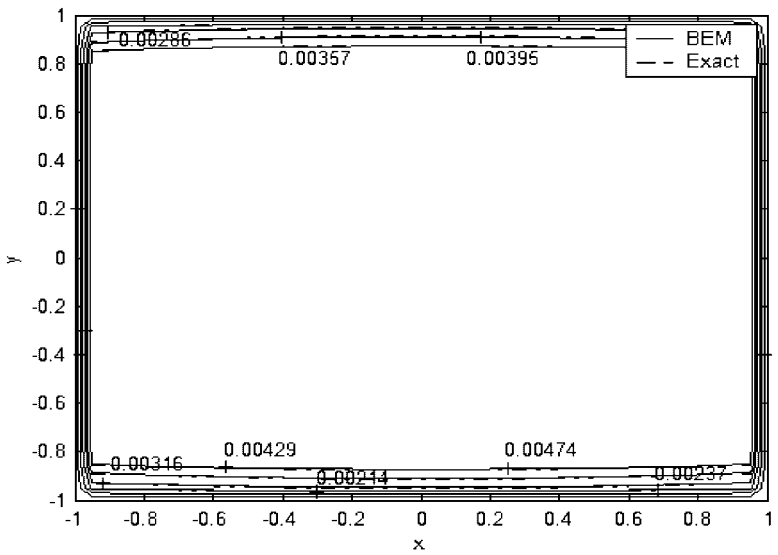

Figure 7. Velocity for $M = 200$, $\tau = 0.15$.

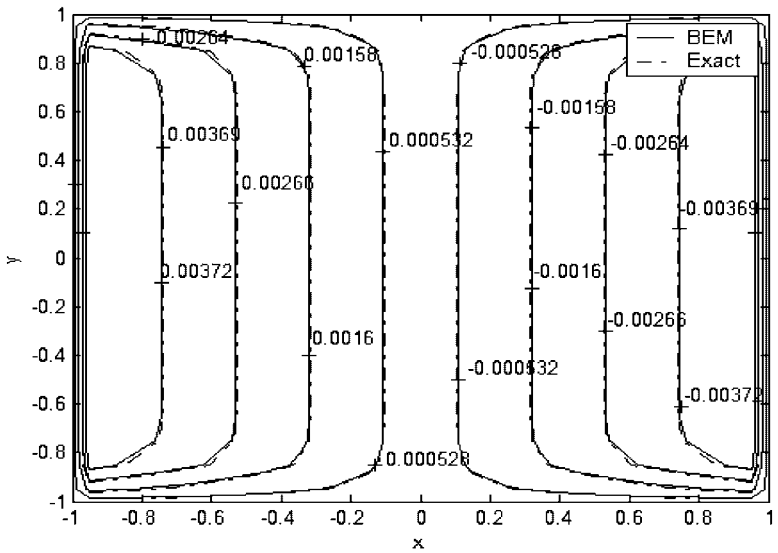

Figure 8. Induced magnetic field for $M = 200$, $\tau = 0.15$.

4.1.2. Problem 2 (Partridge and Sensale [13]). The aim of considering this problem is the similarity with the MHD duct flow equations which will be considered in Section 4.2.

The convection–diffusion equation is given

$$\nabla^2 T - \log\left(\frac{10}{300}\right)\frac{\partial T}{\partial x} = \frac{\partial T}{\partial t}, \quad 0 \leqslant x \leqslant 1, \;\; 0 \leqslant y \leqslant 0.7, \;\; t > 0$$

DOI: 10.1002/fld

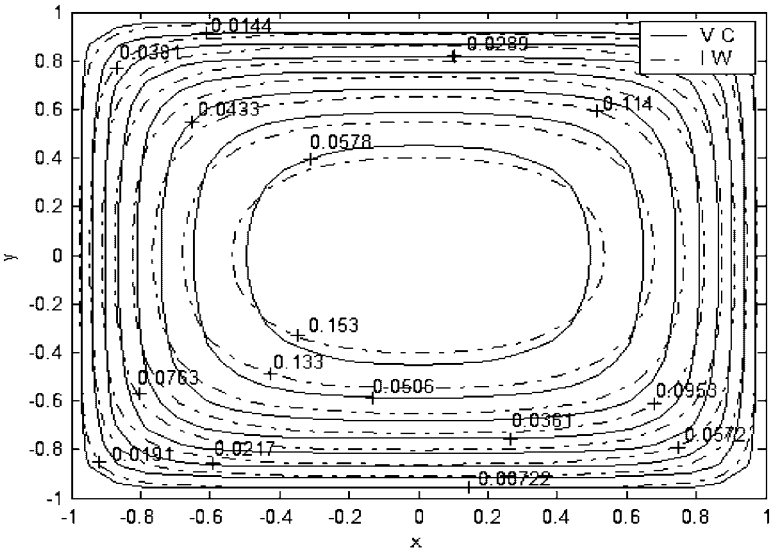

Figure 9. Velocity for $M=5$, $\lambda=0$, $\Delta t=0.5$, $\tau=3.0$.

with the Dirichlet- and Neumann-type boundary conditions

$$\begin{aligned} &T(0, y, t)=300, \\ &T(1, y, t)=10, \end{aligned} \qquad 0\leqslant y\leqslant 0.7,\ t>0$$

$$\begin{aligned} &\frac{\partial T}{\partial n}(x, 0, t)=0, \\ &\frac{\partial T}{\partial n}(x, 0.7, t)=0, \end{aligned} \qquad 0\leqslant x\leqslant 1,\ t>0$$

and the zero initial condition

$$T(x, y, 0)=0$$

We have used again 20 constant boundary elements for the discretization of the boundary of the rectangular domain. The results are obtained at the steady-state $t=8.0$ after four time steps with the time increment $\Delta t=2.0$. Figure 4 shows the agreement of the numerical solution with the steady-state exact solution [14], at the centre point of the interval $0\leqslant y\leqslant 0.7$ along the x-direction. It is clear that for small values of Δt, one needs more iteration to reach the steady-state solution.

4.2. The unsteady MHD duct flow

The unsteady MHD equations defining laminar, viscous flow of an incompressible and electrically conducting fluid in a square duct with variable wall conductivity are solved. The resulting BEM matrix equations are arranged in such a way that we are allowed to solve the equations with the coupled boundary conditions caused by the variable conductivity on the walls.

DOI: 10.1002/fld

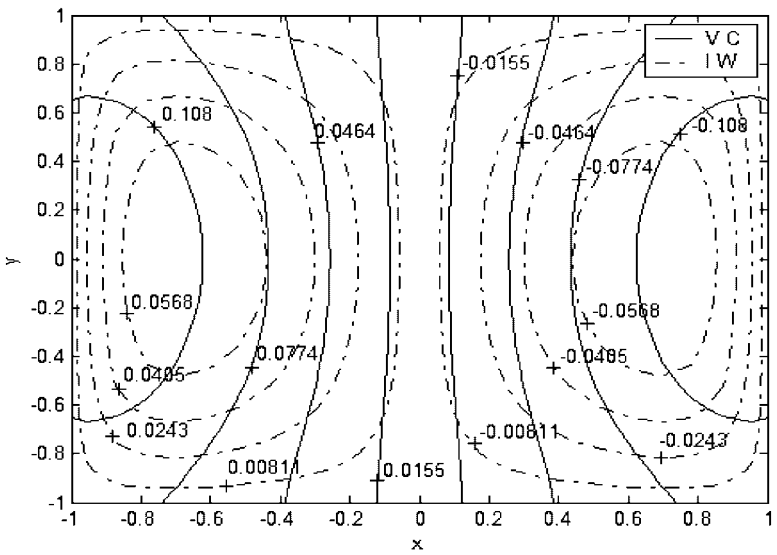

Figure 10. Induced magnetic field for $M = 5$, $\lambda = 0$, $\Delta t = 0.5$, $\tau = 3.0$.

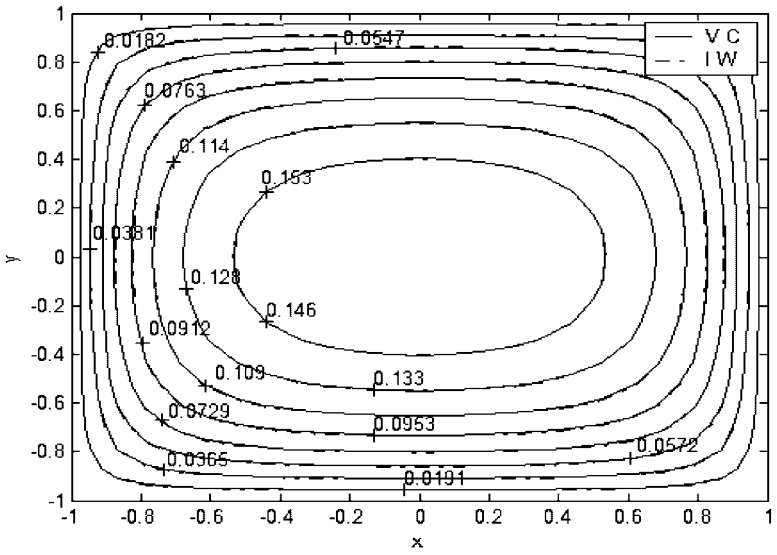

Figure 11. Velocity for $M = 5$, $\lambda = 30$, $\Delta t = 0.5$, $\tau = 2.5$.

To establish the validity of the numerical results, we first solve the unsteady MHD flow of an incompressible fluid in a square duct with insulated walls having a cross-section $-1 \leqslant x, y \leqslant 1$. The numerical results are obtained until reaching the steady-state solution as $\tau \to \infty$ for the time domain $(0, \tau)$ with an accuracy 10^{-5}. In the discretization of the boundary of the duct,

DOI: 10.1002/fld

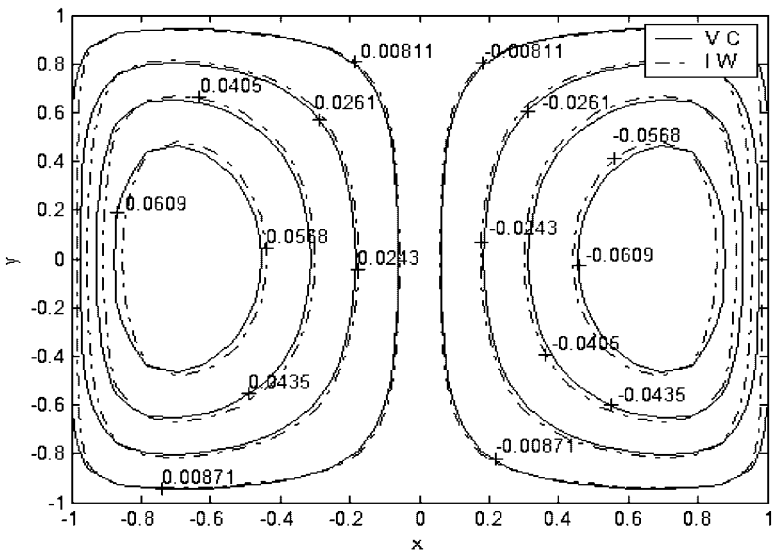

Figure 12. Induced magnetic field for $M = 5$, $\lambda = 30$, $\Delta t = 0.5$, $\tau = 2.5$.

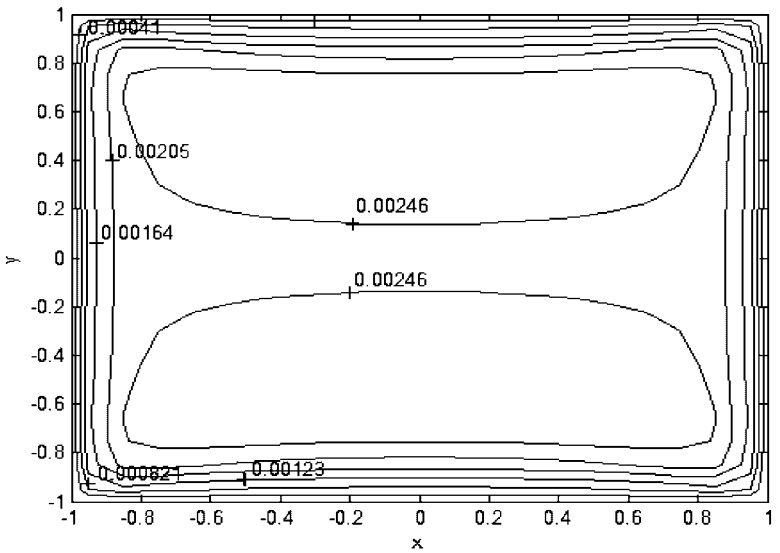

Figure 13. Velocity for $M = 20$, $\lambda = 0$, $\Delta t = 0.5$, $\tau = 2.0$.

we use constant boundary elements ranging from 80 to 100. About 400–625 interior points are used for drawing graphics. In the time domain $(0, \tau)$, we assume again constant variation over each time step. We have obtained the solution of this problem for Hartmann number values up to 300.

DOI: 10.1002/fld

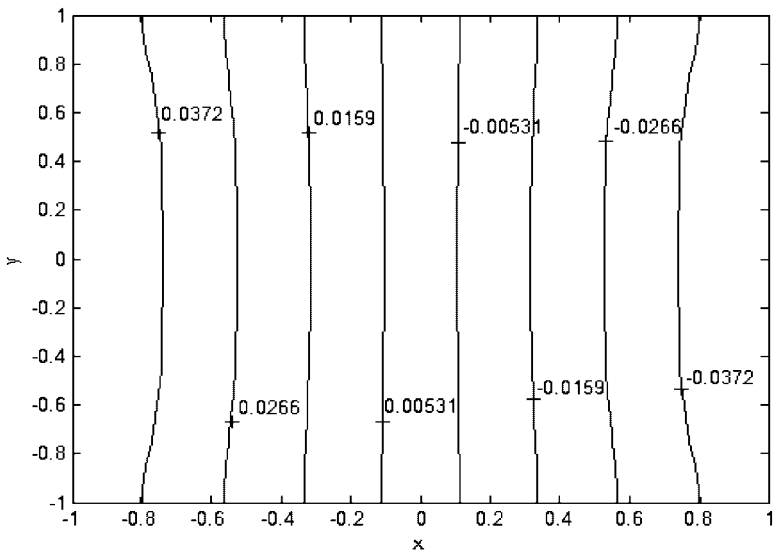

Figure 14. Induced magnetic field for $M = 20$, $\lambda = 0$, $\Delta t = 0.5$, $\tau = 2.0$.

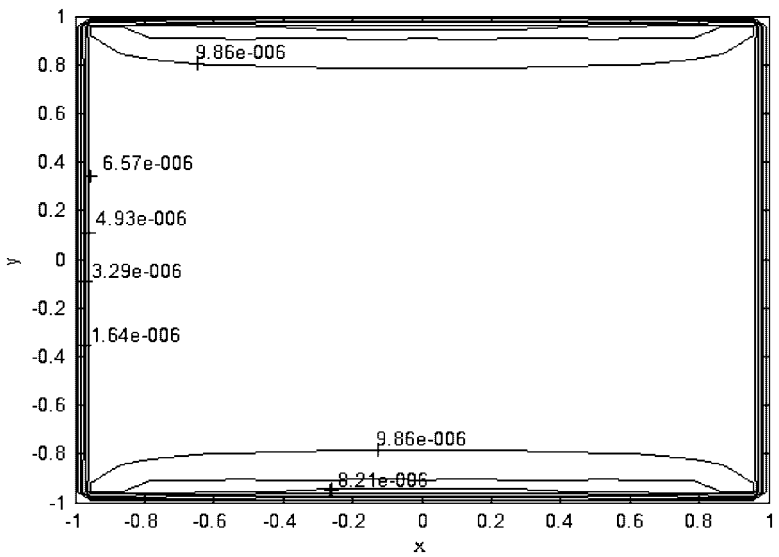

Figure 15. Velocity for $M = 300$, $\lambda = 0$, $\Delta t = 0.03$, $\tau = 0.09$.

In Figures 5–8, the velocity and the induced magnetic field contours presented at the steady state, respectively, for Hartmann numbers $M = 30, 200$. We observe that as M increases we need smaller Δt values to increase the accuracy. However, either with small M (e.g. 30) or larger M (e.g. 200), the number of steps of computations for reaching steady-state (rate of convergence) is

DOI: 10.1002/fld

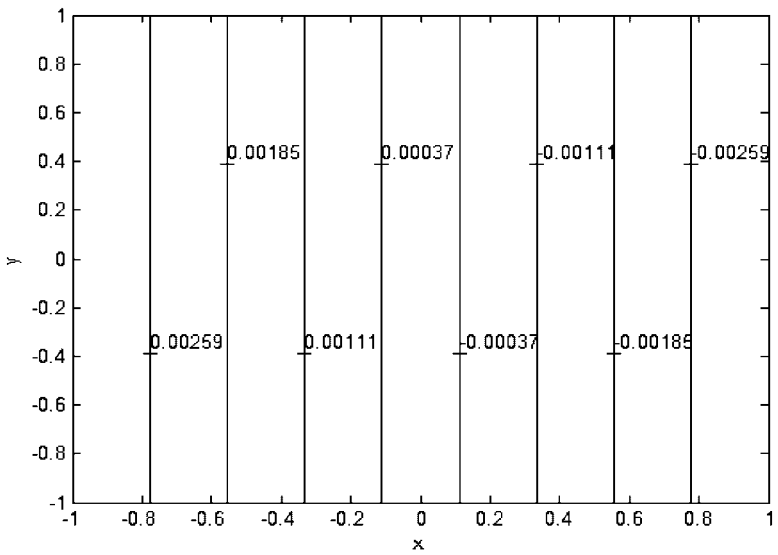

Figure 16. Induced magnetic field for $M = 300$, $\lambda = 0$, $\Delta t = 0.03$, $\tau = 0.09$.

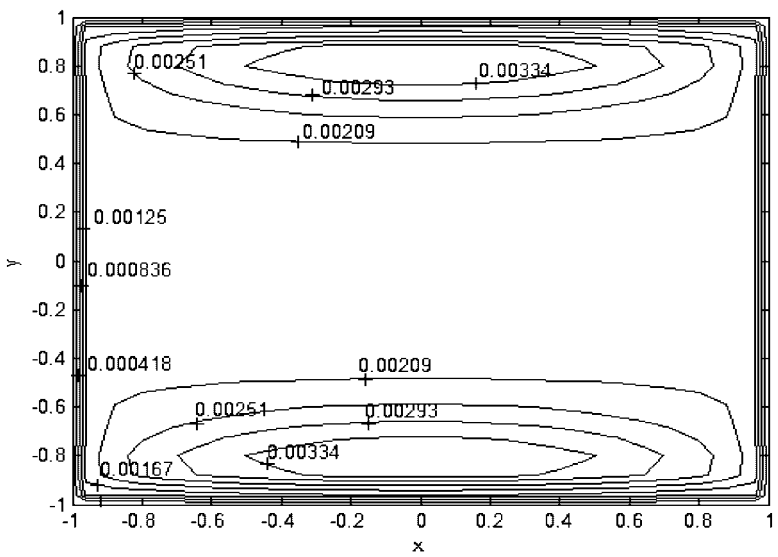

Figure 17. Velocity for $M = 50$, $\lambda = 5$, $\Delta t = 0.5$, $\tau = 1.5$.

always around 3 and 5 with an accuracy 10^{-5}. We can see from Figures 5–8 that our steady-state solutions for the velocity and the induced magnetic field agree very well with the exact solution given by Sherliff [15]. One can also notice from Figures 5 and 7 that as M increases velocity becomes uniform at the centre of the duct and contour values are decreased when getting closer

DOI: 10.1002/fld

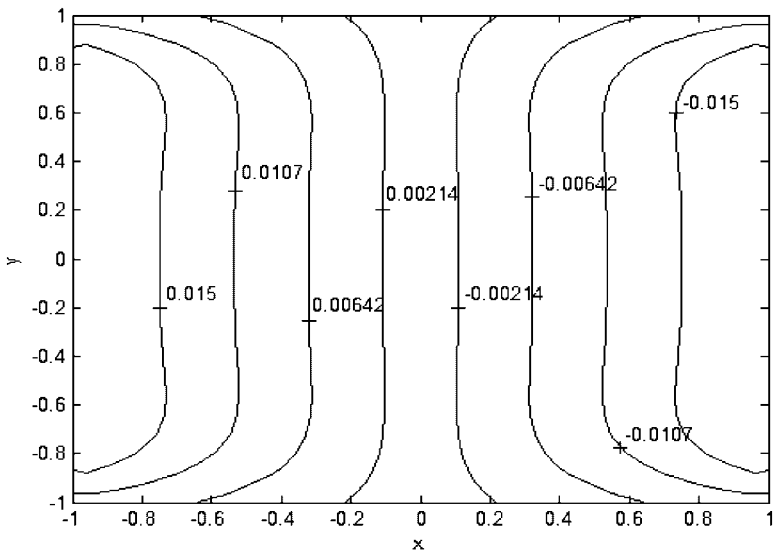

Figure 18. Induced magnetic field for $M = 50$, $\lambda = 5$, $\Delta t = 0.5$, $\tau = 1.5$.

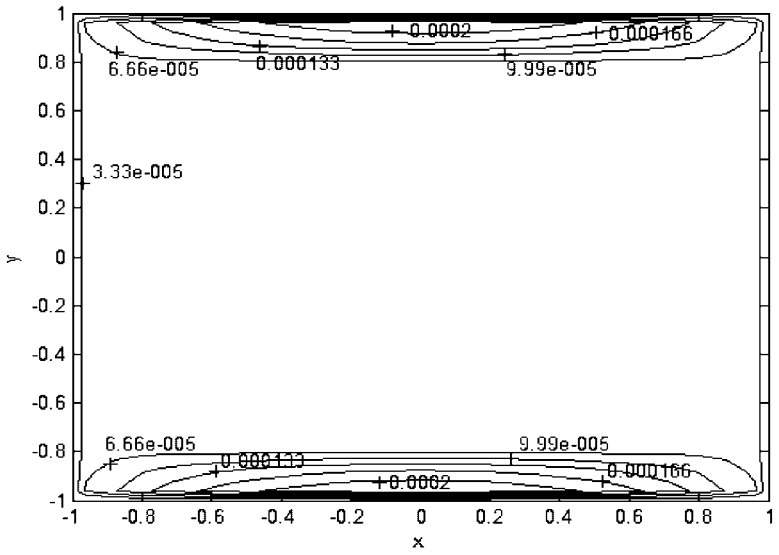

Figure 19. Velocity for $M = 300$, $\lambda = 5$, $\Delta t = 0.03$, $\tau = 0.09$.

to the insulated walls, i.e. V has its maximum value through the centre of the duct and forms boundary layer close to the walls which are the well-known behaviours of the MHD flow.

Now we consider the unsteady MHD flow in a duct with arbitrary conductivity on the walls of the duct. Similar to the insulated wall case, the BEM is employed to the governing equations using

DOI: 10.1002/fld

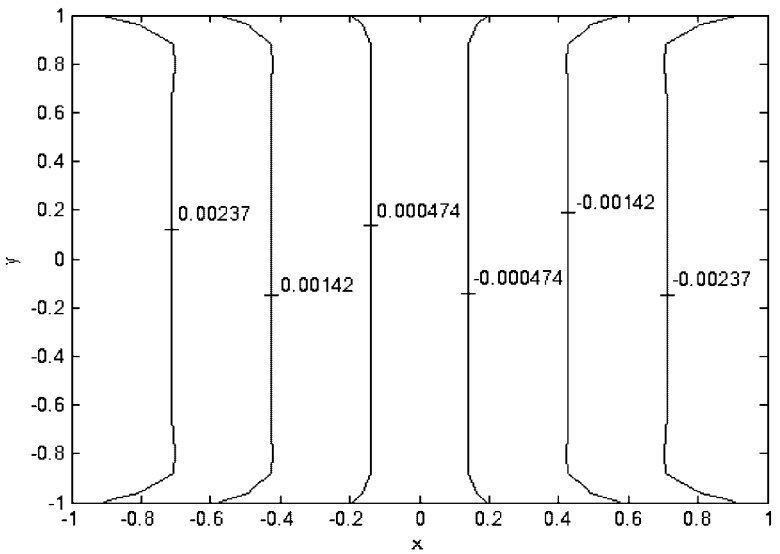

Figure 20. Induced magnetic field for $M = 300$, $\lambda = 5$, $\Delta t = 0.03$, $\tau = 0.09$.

$N = 80, 100$ constant boundary elements with $L = 400, 625$ interior nodes, respectively. Again constant variation is assumed for each time step and the problem is solved on the time domain $(0, \tau)$ as $\tau \to \infty$ up to Hartmann number values 300. Figures 9–12 present a comparison between the behaviour of the numerical results for variable conductivity case ($\lambda = 0, 30$, respectively) and the exact solution for the insulated wall case at the steady state for $M = 5$.

One can observe that when $\lambda = 0$ which is the pure conducting wall case, the induced magnetic field contours are perpendicular to the walls. As λ increases ($\lambda \to \infty$ means the walls are almost insulated) the induced magnetic field contours show the behaviour of solution of MHD flow with insulated walls. In the figures, the notations VC and IW denote variable wall conductivity and insulated wall in the MHD duct flow contours, respectively.

To see the effect of increase in M, we present Figures 13–16 for showing equal velocity and induced magnetic field lines, respectively, for $M = 20, 300$ and for conductivity parameter $\lambda = 0$. In the velocity curves, we notice that the flow is separated symmetrically in the y-direction. This is the effect of applied magnetic field in the direction of x-axis and the pure conductivity of the wall ($\lambda = 0$). As M increases the separation is more pronounced, the fluid is stagnant at the centre region whereas close to the boundaries at $y = \pm 1$ boundary layers are formed.

In Figures 17–20, a similar behaviour for increasing M is observed for velocity and induced magnetic field for $\lambda = 5$. One can notice from Figures 15 and 19 that, the higher the conductivity of the walls is the more stagnant region at the centre region of the duct for the fluid.

5. CONCLUSION

The two-dimensional MHD duct flow equations that are of convection–diffusion type, are solved by using BEM with the time-dependent fundamental solution. The BEM formulation of MHD

DOI: 10.1002/fld

flow equations in a duct with arbitrary wall conductivity is given in such a way that the resulting equations are solved as a whole with coupled boundary conditions. The effects of values of Hartmann number and wall conductivity parameter are visualized in terms of graphics showing the characteristics of MHD duct flow.

REFERENCES

1. Grigoriev MM, Dargush GF. Boundary element methods for transient convective diffusion. Part II: 2D implementation. *Computer Methods in Applied Mechanics and Engineering* 2003; **192**:4299–4312.
2. Grigoriev MM, Dargush GF. Boundary element methods for transient convective diffusion. Part III: Numerical examples. *Computer Methods in Applied Mechanics and Engineering* 2003; **192**:4313–4335.
3. Grigoriev MM, Dargush GF. Efficiency of boundary element methods for time-dependent convective heat diffusion at high Peclet numbers. *Communications in Numerical Methods in Engineering* 2005; **21**:149–161.
4. DeSilva SJ, Chan CL, Chandra A, Lim J. Boundary element method analysis for the transient conduction–convection in 2-D with spatially variable convective velocity. *Applied Mathematical Modelling* 1998; **22**:81–112.
5. Singh B, Lal J. Finite element method for unsteady MHD flow through pipes with arbitrary wall conductivity. *International Journal for Numerical Methods in Fluids* 1984; **4**:291–302.
6. Salah NB, Soulaimani A, Habashi WG. A finite element method for magnetohydrodynamic. *Computer Methods in Applied Mechanics and Engineering* 2001; **190**:5867–5892.
7. Seungsoo L, Dulikravich GS. Magnetohydrodynamic steady flow computation in three dimensions. *International Journal for Numerical Methods in Fluids* 1991; **13**:917–936.
8. Sheu TWH, Lin RK. Development of a convection–diffusion–reaction magnetohydrodynamic solver on nonstaggered grids. *International Journal for Numerical Methods in Fluids* 2004; **45**:1209–1233.
9. Bozkaya C, Tezer-Sezgin M. Boundary element method solution of unsteady magnetohydrodynamic duct flow with differential quadrature time integration scheme. *International Journal for Numerical Methods in Fluids* 2006; **51**:567–584.
10. Carslaw HS, Jaeger JC. *Conduction of Heat in Solids* (2nd edn). Clarendon Press: Oxford, 1959.
11. Brebbia CA, Telles JCF, Wrobel LC. *Boundary Element Techniques*. Springer: Berlin, 1984.
12. Dragos L. *Magneto-fluid Dynamics*. Academic Press: England, 1975.
13. Partridge PW, Sensale B. The method of fundamental solutions with dual reciprocity for diffusion and diffusion–convection using subdomains. *Engineering Analysis with Boundary Elements* 2000; **24**:633–641.
14. DeFigueiredo DB. *Boundary Element Analysis of Convection Diffusion Problems*. Lecture Notes in Engineering Series. Springer: Berlin, 1991.
15. Sherliff JA. The motion of conducting fluids in pipes under transverse fields. *Proceedings of the Cambridge Philosophical Society*, vol. 49, 1953; 136–144.

DOI: 10.1002/fld